Triphenylphosphine-functionalized core-cross-linked micelles and nanogels with a polycationic outer shell: synthesis and application in rhodium-catalyzed biphasic hydrogenations

Hui Wang, Lorenzo Vendrame, Christophe Fliedel, Si Chen, Florence Gayet, Franck d'Agosto, Muriel Lansalot, Eric Manoury, Rinaldo Poli

Triphenylphosphine-functionalized core-cross-linked micelles and nanogels with a polycationic outer shell: synthesis and application in rhodium-catalyzed biphasic hydrogenations

Hui Wang,[a] Lorenzo Vendrame,[a] Christophe Fliedel,[a] Si Chen,[a] Florence Gayet,[a] Franck D'Agosto,[b] Muriel Lansalot,[b] Eric Manoury,[a] Rinaldo Poli*[a][c]

[a] Ms. H. Wang, Mr. L. Vendrame, Dr. C. Fliedel, Dr. S. Chen, Dr. F. Gayet, Dr. E. Manoury, Prof. R. Poli
CNRS, LCC (Laboratoire de Chimie de Coordination), Université de Toulouse, UPS, INPT
205 route de Narbonne, BP 44099, F-31077 Toulouse Cedex 4, France
E-mail: rinaldo.poli@lcc-toulouse.fr

[b] Dr. F. D'Agosto, Dr. M. Lansalot
Univ Lyon, Université Claude Bernard Lyon 1, CPE Lyon, CNRS, UMR 5265, Chemistry, Catalysis, Polymers and Processes (C2P2)
43 Bd du 11 Novembre 1918, 69616 Villeurbanne, France

[c] Prof. R. Poli
Institut Universitaire de France,
1 rue Descartes, 75231 Paris Cedex 05, France

Supporting information for this article is given via a link at the end of the document.

Abstract: Unimolecular amphiphilic nanoreactors with a poly(4-vinyl-*N*-methylpyridinium iodide) (P4VPMe$^+$I$^-$) polycationic outer shell and two different architectures (core-crosslinked micelles, CCM, and nanogels, NG), with narrow size distributions around 130-150 nm in diameter, were synthesized by RAFT polymerization from an R_0-4VPMe$^+$I$^-_{140}$-*b*-S_{50}-SC(S)SPr macroRAFT agent by either chain extension with a long (300 monomer units) hydrophobic polystyrene-based block followed by crosslinking with diethylene glycol dimethacrylate (DEGDMA) for the CCM particles, or by simultaneous chain extension and crosslinking for the NG particles. A core-anchored triphenylphosphine (TPP) ligand functionality was introduced by using 4-diphenylphosphinostyrene (DPPS) as a comonomer (5-20% mol/mol) in the chain extension (for CCM) or chain extension/crosslinking (for NG) step. The products were directly obtained as stable colloidal dispersions in water (latexes). After loading with $[RhCl(COD)]_2$ to yield [RhCl(COD)(TPP@CCM)] or [RhCl(COD)(TPP@NG)], respectively, the polymers were used as polymeric nanoreactors in the Rh-catalyzed aqueous biphasic hydrogenation of the model substrates styrene and 1-octene, either neat (for styrene) or in an organic solvent (toluene or 1-nonanol). All hydrogenations were rapid (TOF up to 300 h^{-1}) at 25°C and 20 bar of H_2 pressure, the biphasic mixture rapidly decanted at the end of the reaction (< 2 min), the Rh loss was negligible (< 0.1 ppm in the recovered organic phase), and the catalyst phase could be recycled 10 times without significant loss of catalytic activity.

Introduction

Transformations requiring expensive molecular catalysts (metals and/or ligands) can only be implemented at the industrial level if the catalyst can be efficiently separated from the reaction products and recycled. An attractive way to achieve this is through the liquid/liquid biphasic implementation, involving catalyst confinement in a different liquid medium than the reagents and products and allowing catalyst separation and recovery by decantation. Water is a particularly attractive medium for catalyst confinement because it is inexpensive and non-toxic.[1] The best-known aqueous biphasic industrial process is probably the Ruhrchemie/Rhone-Poulenc (RRP) rhodium-catalyzed hydroformylation of light olefin (propene, butene).[2] In liquid/liquid biphasic protocols, the catalyzed transformation may take place in one of four distinct environments: (*i*) in the catalyst phase, if the substrates have non-zero solubility in the catalyst medium (for instance, as in the RRP process); (*ii*) in the substrate/product phase, if the catalyst can be transported to that phase by a temperature stimulus (thermomorphic catalysis)[3] or by a phase transfer agent; (*iii*) at the interface, if neither component is sufficiently soluble in the other component phase;[4] and finally (*iv*) within the homogeneous environment of catalytic nanoreactors such as functionalized micelles. In aqueous biphasic protocols, very hydrophobic substrates do not have sufficient solubility in water, leading to severe mass transport limitations for the implementation of type (*i*) and hence require using one of the other methods, (*ii*), (*iii*) or (*iv*). The last protocol has recently attracted considerable attention, because kinetically stable micelles can be easily formed by assembling amphiphilic diblock copolymers in water.[5] However, recognized limitations of this approach are micellar swelling, which leads to slow-decanting emulsions, and equilibria with single chains, which leads to catalyst leaching.

We have recently developed new polymeric supports for aqueous biphasic catalysis, consisting of core-crosslinked micelles (CCM)[6] and nanogels (NG),[7] see Figure 1. These are unimolecular nanosized polymeric architectures and thus immune from extensive swelling and particle-chain equilibria. The catalyst is covalently anchored within the hydrophobic core and the particles remain confined in the water phase thanks to a hydrophilic outer shell. The CCM and NG particles differ by the core architecture. In the former, amphiphilic diblock macromolecules with hydrophobic and ligand-functionalized linear chains are crosslinked at the end of the hydrophobic blocks in the final synthetic step, whereas the latter are built by simultaneous chain extension, functionalization and crosslinking from a hydrophilic macromolecular chain transfer agent. The main differences between CCM and NG is that the first one features crosslinking only in the central part of the core and the ligands are placed on flexible arms outside the crosslinked area, whereas the latter has an almost entirely crosslinked core with the ligands incorporated inside it. The technique that efficiently allowed us to develop particle with controlled size and

architecture is reversible addition-fragmentation chain transfer (RAFT) polymerization,[8] implemented under aqueous conditions and resulting in "polymerization-induced self-assembly" (PISA).[9] Other types of unimolecular polymer-based catalytic nanoreactors, which are crosslinked at the level of either the outer shell, the core, or an inner corona, have also been developed by other groups,[10] though they were not employed under aqueous biphasic conditions with particular attention to catalyst leaching and recycling.

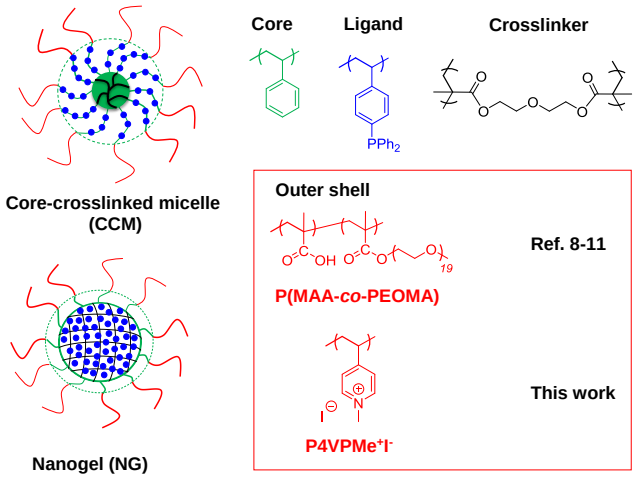

Figure 1. Architecture and composition of the core-crosslinked micelles (CCM) and nanogel (NG) particles.

Our first generation polymers were constructed with a neutral hydrophilic shell based on randomly copolymerized methacrylic acid (MAA) and poly(ethylene oxide) methyl ether methacrylate (PEOMA). The hydrophobic core consisted of polystyrene (PS), where the desired ligand was introduced by copolymerization of a suitably functionalized styrene (*e.g.* 4-diphenylphosphinostyrene, DPPS, to yield PS-anchored triphenylphosphine functions) and diethylene glycol dimethacrylate (DEGDMA) was used as crosslinker.[6-7, 11] After coordination of a suitable precatalyst, these polymeric nanoreactors proved efficient in the aqueous biphasic rhodium-catalyzed hydroformylation of a model water insoluble α-olefin (1-octene)[6a, c, 7, 11a] and in the rhodium-catalyzed hydrogenation of 1-octene and styrene,[11d] and their recyclability was demonstrated. However, these systems had two limitations, negating their possible implementation for large scale applications: (*i*) after removal from the reaction medium (stirring at 1200 rpm at 80°C for two hours) the phase separation was rather slow, requiring several hours to yield an optically transparent organic phase; (*ii*) the presence of a significant Rh concentration in the organic phase was revealed by ICP-MS. The Rh leaching was demonstrated to be associated to the presence of polymeric nanoreactors in the recovered organic phase (DLS measurements) and not to loss of Rh molecules from the nanoreactor core. In addition, the amount of leached Rh was shown to be stirring- and architecture-dependent (1.7-2.5 ppm for CCM[6c] or 0.6 ppm for NG[7] at 1200 rpm; sharp leaching increase for the CCM as the stirring rate was increased up to 1600 rpm).[6c, 7] Furthermore, the DLS of the recovered organic phase showed that the nanoreactors in the organic phase had undergone irreversible agglomeration (more extensive for greater stirring rates) and were kinetically stabilized in the organic phase. The agglomeration phenomenon was investigated in greater detail and proven to be associated to a reversible particle-particle interpenetration and subsequent irreversible interparticle arm-arm coupling via ligand exchange at the Rh center.[11c] All these phenomena were recognized to be promoted by the temperature-sensitive behavior of the neutral P(MAA-*co*-PEOMA) blocks. At higher temperatures, the outer-shell becomes less hydrophilic, favoring transfer to the organic phase, and more lipophilic, favoring particle-particle interpenetration.

In order to correct these problems, we have thus developed a second-generation nanoreactor scaffold, containing a hydrophilic outer shell that does not suffer from temperature-sensitive behavior. As a first choice, we have selected a polycationic shell that contains quaternized (methylated) 4-vinylpyridine (4VP) units, -[CH_2-CH(4-$C_5H_4NMe^+I^-$)]- (4VPMe^+I^-). In a recent contribution, we have described the optimized synthesis of both CCM and NG particles with a PS hydrophobic core (without anchored ligand functionalities) and DEGDMA-based crosslinking.[12] After surmounting a few synthetic obstacles, particles of controlled architecture, narrow size distribution and quantitative arm crosslinking could be obtained.

In the present contribution, we report the synthesis and characterization of triphenylphosphine-functionalized versions of these particles (TPP@CCM and TPP@NG; see Figure 1), their coordination chemistry with $[RhCl(COD)]_2$, an investigation of the interparticle metal migration, and finally their application in the aqueous biphasic hydrogenation of styrene and 1-octene as model substrates, demonstrating their superior performance in all respects (activity, speed of decantation, leaching) relatively to the first-generation nanoreactors.

Results and Discussion

(a) Polymer syntheses

The optimized syntheses of the polymers (see Figure 2) started from the diblock macroRAFT agent R_0-(4VPMe^+I^-)$_{140}$-*b*-S_{50}-SC(S)SPr, already reported in our recent contribution,[12] which was obtained in three steps: (*i*) homogeneous RAFT polymerization of 4VP in water/ethanol with 4- cyano-4-thiothiopropylsulfanyl pentanoic acid (CTPPA, or R_0-SC(S)SPr with R_0 = -C(CH_3)(CN)CH_2CH_2COOH) as RAFT agent and 4,4'-azobis(4-cyanopentanoic acid) (ACPA) as initiator, to yield R_0-4VP_{140}-SC(S)SPr; (*ii*) chain extension with styrene, which leads to PISA, with formation of a latex of R_0-4VP_{140}-*b*-S_{50}-SC(S)SPr; (*iii*) reaction with MeI/DMF, leading to the desired macroRAFT agent, which was isolated as a yellow powder containing residual DMF of solvation (R_0-(4VPMe^+I^-)$_{140}$-*b*-S_{50}-SC(S)SPr·34DMF). All steps led to narrowly distributed molar masses attesting the control of the polymerization.[12]

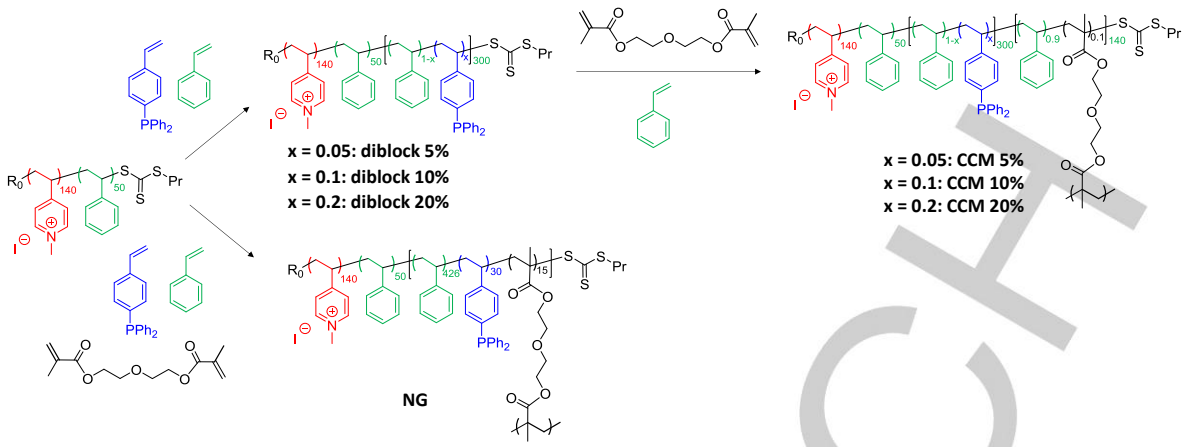

Figure 2. Synthesis of the triphenylphosphine-functionalized CCM and NG particles with an outer P4VPMe$^+$I$^-$ hydrophilic shell.

For the CCM synthesis, this macroRAFT agent was first chain-extended with the appropriate mixture of styrene and diphenylphosphinostyrene (DPPS), yielding latexes of the corresponding R_0-(4VPMe$^+$I$^-$)$_{140}$-*b*-S$_{50}$-*b*-(S$_{1-x}$-*co*-DPPS$_x$)$_{300}$-SC(S)SPr amphiphilic linear chains. Three versions were prepared with x = 0.05 (**diblock 5%**, with an average of 15 ligands per chain), 0.1 (**diblock 10%**, 30 ligands per chain) and 0.2 (**diblock 20%**, 60 ligands per chain). These polymers were then crosslinked with a DEGDMA/S (10:90) mixture in the final step to afford R_0-(4VPMe$^+$I$^-$)$_{140}$-*b*-S$_{50}$-*b*-(S$_{1-x}$-*co*-DPPS$_x$)$_{300}$-*b*-(S$_{0.9}$-*co*-DEGDMA$_{0.1}$)$_{140}$-SC(S)SPr (**CCM 5%**, **CCM 10%** and **CCM 20%**, respectively). The latex of the NG particles (**NG**) was obtained in a single step, copolymerizing simultaneously styrene, the ligand-functionalized DPPS monomer and the DEGDMA crosslinker. Only a version containing on average 30 DPPS monomers per chain, R_0-(4VPMe$^+$I$^-$)$_{140}$-*b*-S$_{50}$-*b*-(S$_{426}$-*co*-DPPS$_{30}$-*co*-DEGDMA$_{15}$)-SC(S)SPr, like the **CCM 10%** product, was developed, although the total amount of styrene and crosslinker per chain is greater and therefore the overall ligand concentration in the hydrophobic core is intermediate between those of **CCM 10%** and **CCM 5%**. All the latexes obtained were low viscosity colloidal dispersions, in spite of the high polymer content (16-24% in weight), with a milky aspect. They were all stable in time, giving no evidence of destabilization or gradient development over several months. The particle sizes were characterized by DLS and TEM and the corresponding polymers were characterized by ^{1}H and ^{31}P NMR spectrometry. The particle size was too large to allow meaningful SEC or NMR-DOSY analyses.

The ^{1}H NMR spectra obtained after diluting an aliquot of the latex into different deuterated solvents are collected in Figures S1-5. Dilution with DMSO-d_6 allowed monitoring the monomer consumption but the particle core resonances were not revealed, since DMSO is not a good solvent for PS. On the other hand, after core swelling with $CDCl_3$ – a good solvent for PS – and dilution into D_2O, the core resonances became observable. Like for the previously published latexes of the related CCM and NG particles with the neutral P(MAA-*co*-PEOMA) shell,[6c, 7] resonances that could be unambiguously attributed to the DEGDMA crosslinker could not be clearly distinguished, probably because of the small amount of this monomer. It is also worth pointing out that the DEGDMA protons, being close to the polymer crosslinking points, have more restricted mobility and their resonances are therefore expected to be broader.

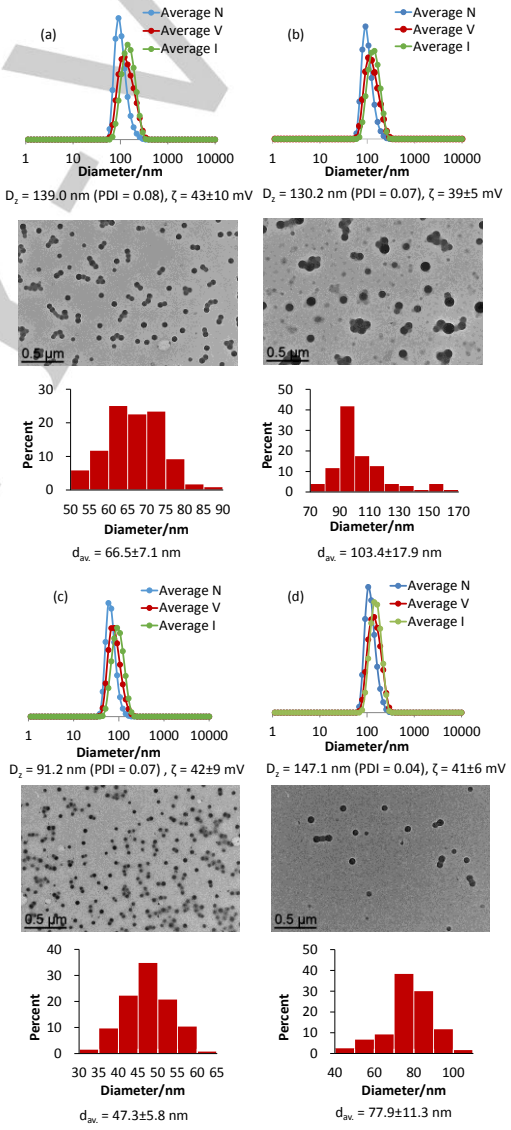

Figure 3. DLS with D_z, PDI and zeta potential values (above), representative TEM images (middle) and frequency analysis of the diameters with average and standard deviation from the TEM images (below, > 100 measured particles) for: (a) **CCM 5%**; (b) **CCM 10%**; (c) **CCM 20%**; (d) **NG**. All reported DLS data were obtained on unfiltered solutions.

The DPPS incorporation in the polymer core cannot be assessed from the ^{1}H NMR spectra because the corresponding resonances cannot be distinguished from those of the styrene units. However, the presence of core-linked DPPS units was clearly indicated by a relatively broad resonance in the ^{31}P NMR spectrum at ca. -6.5 ppm, slightly shifted from the resonance of the precursor DPPS in the same $CDCl_3$ solvent (Figure S6). The same broadening and resonance shift was previously observed for the incorporation of DPPS in the equivalent polymers with the neutral outer shell.[6c, 7] The DLS and TEM analyses (Figure 3) showed that all obtained polymers have spherical morphology, with average diameter in the 130-150 nm range and narrow size distributions. The zeta potentials are positive and as expected essentially equivalent, with experimental error, for all polymers. In addition, DLS measurements of **CCM 5%**, **CCM 10%** and **NG** after freeze-drying and redispersion in a DMSO-toluene 80:20 (v/v) mixture revealed the absence of uncrosslinked arms (see Figure S7). Indeed, this solvent mixture is able to solvate both blocks and would reveal the presence of single chains at smaller diameters, as previously demonstrated for the analogous DPPS-free diblock.[12] The particle diameters revealed by the TEM images are a bit smaller than those obtained from the DLS data (see the frequency analysis in Figure 3, bottom part), because the TEM measures the objects after deposition and drying on the grid support, whereas the DLS data are obtained on the solvated particles and thus reflect the diameter expansion by the hydrophilic shell solvation.

An exploration by TEM analysis (details in the SI, Table S1) of the CCM morphology dependence on the hydrophilic and hydrophobic block molar masses showed that a reduction of the hydrophilic block molar mass (72 or 56 4VPMe^{+}I^{-} units), while maintaining a similar molar mass for the hydrophobic part, led to mixtures of cylindrical and spherical micelles for the linear amphiphilic intermediate. This switch in morphology is consistent with the behavior of block copolymers with higher molar mass hydrophobic block and self-assembling during a PISA process.[9d] It indirectly attests the control of the polymerization during chain extension, indicating that well-defined block copolymers were achieved. Interestingly, rearrangement to spherical CCM particles occurred when using greater amounts of S/DEGDMA in the crosslinking step. The corresponding strong plasticization of the core of the nano-objects probably helps the reorganization of the block copolymers during this step into spherical morphologies, rapidly locked by the crosslinking reaction. Shortening the hydrophobic chain molar mass (e.g. R_0-(4VPMe^{+}I^{-})$_{56}$-*b*-S$_{32}$-*b*-(S$_{1-x}$-*co*-DPPS$_x$)$_{118}$-) ensured a spherical morphology for the intermediate micelles, although the final crosslinked objects had a less well-defined morphology. The most homogeneous spherical morphology for both the intermediate micelles and the final CCM particles was obtained when using the longer outer block (140-150 4VPMe^{+}I^{-} monomer units). Since the spherical morphology seems most suitable for applications as nanoreactors in biphasic catalysis, the optimum balance of hydrophilic and hydrophilic parts of the CCM nanoreactors was fixed as ca. 150 and 300 before crosslinking, and an overall equivalent ratio of hydrophilic/hydrophobic parts was maintained for the NG synthesis.

In terms of swelling capacity and mass transport, these polymers do not show any substantial difference relative to the equivalent ones with the neutral P(MAA-*co*-PEOMA) outer shell: the incorporation of swelling solvents (toluene or chloroform) was quite rapid (< 1 min) upon shaking the biphasic mixture, as visually assessed by the change of the relative phase volumes, and gave rise to an average diameter increase while maintaining narrow size dispersions (Figure S8). Therefore, changing the hydrophilic shell from neutral P(MAA-*co*-PEOMA) to polycationic P4VPMe^{+}I^{-} does not negatively affect the migration of neutral organic compounds from an external continuous phase to the nanoreactor core.

(b) [RhCl(COD)]$_2$ precatalyst coordination and migration studies

Using the same protocol optimized in previous contributions,[11d, 13] complex [RhCl(COD)]$_2$ was introduced into the nanoreactor cores after pre-swelling the polymer particles with toluene. Upon equilibrating the latex phase with a toluene solution of the metal complex under vigorous stirring at room temperature, the Rh complex was transferred into the nanoreactor cores quantitatively within 30 min, as optically assessed by the transfer of the complex orange color from the organic to the aqueous phase. Hence, the polycationic nature of the outer shell also makes no opposition to the metal complex migration. Spectroscopic evidence of metal complexation, leading to the core-anchored [RhCl(COD)(TPP@CCM)] functions, was possible only when the polymers were quantitatively charged with the metal complex (P:Rh = 1:1). The free TPP resonance at -6.5 ppm was fully replaced by a doublet at 32.2 ppm assigned to the Rh-coordinated TPP (e.g. see the spectra for the **CCM 10%** particles in Figure 4). Although relatively broad because of the increased correlation time in the polymeric environment, the Rh coupling is clearly discernible with $J_{PRh} \approx 150$ Hz, consistent with previous studies.[6a, 7, 11a-c, 13] These spectral parameters agree well with those reported for the molecular model (31.5 ppm, J = 152 Hz)[14] and for the same complex anchored to the equivalent neutral-shell polymer (29.3 ppm, J = 150 Hz).[13] The spectra for the Rh-charged particles at higher P:Rh ratios (2:1 or 4:1) gave no observable signal because of further broadening by the rapid degenerative phosphine exchange, as previously described for the equivalent neutral-shell polymers.[13]

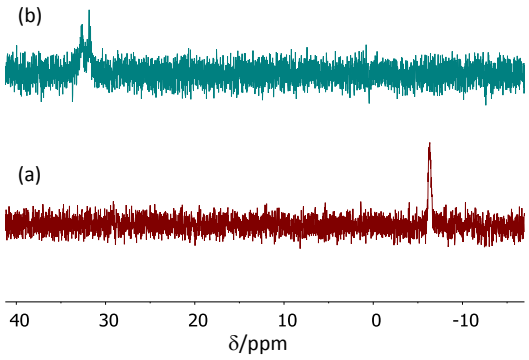

Figure 4. ^{31}P NMR spectrum for the toluene-swollen **CCM 10%** latex, before (a) and after (b) equilibration with a [RhCl(COD)]$_2$ toluene solution at a P:Rh ratio of 1:1.

In our previous work with the equivalent neutral-shell nanoreactors, the ^{31}P signal disappearance at higher P:Rh ratios could be used to demonstrate a fast metal migration between

cores of different macromolecules. A different complex, [Rh(acac)(CO)$_2$], was used in that case, yielding [Rh(acac)-(CO)(TPP)] upon introduction in the CCM core. When two TPP@CCM latexes, one pristine and one 100% loaded with the Rh complex, were mixed in a 1:1 ratio (thus with a global P:Rh ratio of 2:1), the ^{31}P signals disappeared immediately. This phenomenon was proven to result from phosphine exchange reactions,[11c] by analogy with the behaviour in homogeneous solution,[15] which requires reversible particle interpenetration and core-core contact. Indeed, the migration was stopped at high pH (13.6), because the Coulombic repulsion between the polyanionic shells generated by deprotonation of the methacrylic acid units stops the interpenetration process. The present polycationic shell polymers proved to be equally capable of stopping the metal migration, as demonstrated by the persistence of the simultaneously observable ^{31}P NMR resonances for the free and coordinated TPP ligands in the 1:1 mixture of pristine and 100% loaded TPP@CCM latexes (the P-richer **CCM 20%** sample was used for this experiment), even after stirring the mixture for over 1 week at room temperature, see Figure 5. This demonstrates the efficient confinement of the metal complex within the core of the nanoreactor in which it has initially been anchored. Obviously, intraparticle phosphine exchange processes continue to take place, as shown by the absence of the ^{31}P resonance for partially loaded latexes.

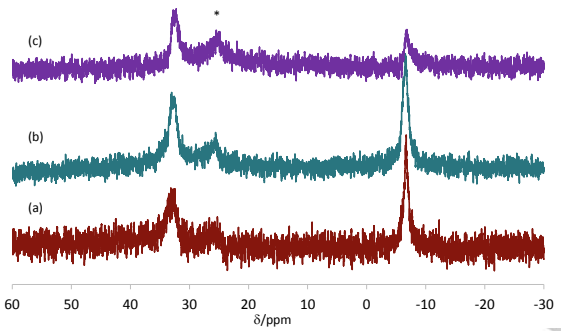

Figure 5. ^{31}P NMR spectra recorded at different times after mixing equivalent amounts of **CCM 20%** latexes with 0 and 100% Rh loadings, and stirring at room temperature: (a) 1.5 h; (b) 7 h; (c) 1 week. The starred resonance corresponds to phosphine oxide.

It is interesting to compare the monitoring of Figure 5 with that of the corresponding experiment for the polymer with the neutral P(MAA-*co*-PEOMA) shell at high pH. In the latter case, even though the immediate exchange via core-core contact was stopped, a slow change (complete in ca. 10 h at room temperature) took place with formation of a single product, [Rh(OH)(CO)(TPP@CCM)$_2$], indicating a slower metal migration accompanied by a chemical transformation. This phenomenon was shown to involve Rh extraction from the polymer-bound [Rh(acac)(CO)(TPP@CCM)] complex by OH^- and migration through the continuous aqueous phase, presumably as anionic [Rh(acac)(OH)(CO)]$^-$. In the present case, the insignificant change of the NMR spectrum over 1 week indicates the absence not only of core-core contact but also of any metal migration through the continuous phase. Namely, the Rh metal does not leach out of the nanoreactor core.

(c) Biphasic catalytic hydrogenations

All nanoreactors were used to catalyze the hydrogenation of styrene and 1-octene as representative aromatic and aliphatic unsaturated substrates. Two different protocols were used for styrene, with the substrate introduced either neat or diluted into 1-nonanol. For 1-octene, the neat substrate could not be used because it is not a good solvent for the polystyrene core and is therefore not able to swell it. The catalytic application required substrate dilution into a good solvent for polystyrene. The choice of 1-nonanol was guided by our previous optimization study of the same biphasic catalytic reaction with the neutral-shell polymer,[11d] where a first attempt with use of toluene (a better solvent for polystyrene) led to coagulation because of particle-particle coupling. This phenomenon was interpreted as resulting from the nanoreactor interpenetration, allowing the coordinatively unsaturated Rh center in catalytic intermediates to bind to TPP ligands of different particles. Using 1-nonanol (sparingly soluble in water, good solvent for polystyrene, and able to stabilize transient unsaturated forms of the catalytically active species by coordination) led to successful implementation of the reaction with no polymer coagulation and rapid phase decantation. Although the polycationic shell of the new nanoreactors should stop the particle interpenetration, the use of 1-nonanol was initially maintained in order to compare the performances of the cationic and neutral shell polymeric nanoreactors.

c.1. Hydrogenation of styrene in 1-nonanol.

A first exploratory investigation was carried out to assess the effect of various parameters on the catalytic efficiency: P:Rh ratio (1:1, 2:1 and 4:1, for the **CCM 10%** nanoreactor), P content in the CCM (5% *vs.* 10%) and nanoreactor architecture (CCM *vs.* NG). In all cases, decantation was very rapid, as previously observed for the equivalent hydrogenation with the neutral-shell nanoreactors. For each experiment, the only detected product was ethylbenzene, showing selective hydrogenation of the vinyl function as expected for a molecular Rh catalyst. The generation of Rh nanoparticles, which is known to occur from Rh^I precursor in the absence of stabilizing π-acidic ligands, would also lead to significant ring hydrogenation, as shown in previous reports of the reduction of arenes[16] including styrene.[17] Using a 10% (v/v) styrene solution in 1-nonanol, a styrene/Rh ratio of 200, and an H_2 pressure of 20 bar at 25°C, quantitative substrate conversion was achieved after ca. 5 h of stirring in all cases. A representative conversion *vs.* time plot for the **CCM 10%** system with a P:Rh ratio of 4:1 is shown in Figure 6 and the full data for all systems are collected in the SI (Table S2). Considering the need of single-point kinetic monitorings and the associated experimental errors, leading to a relatively large scatter of the data (see Figure S9), no clear trends can be derived from a comparison of the data obtained under different experimental conditions. Thus, all subsequent experiments made use of the **CCM 10%** scaffold with a P:Rh ratio of 4:1. From the initial slope in Figure 6, the TOF can be roughly estimated as 70 h^{-1}.

The performance of the **CCM 10%** biphasic system was also compared with the homogeneous system operated under identical conditions. The two systems differ only by the biphasic *vs.* monophasic nature, introducing the potential effect of mass transport on the reaction kinetics, and by the effective catalyst concentration. Indeed, for the biphasic nanoreactor implementation, all the Rh active centers are concentrated within

the nanoreactor cores, the total volume of which is much smaller than the total volume of the organic phase. From the polymer content in the latex, the nanoreactor swelling capacity and the amounts used in the catalytic experiments, the effectively catalyst concentration in the nanoreactors can be roughly estimated as 2.3 times greater than that of the homogeneous system. The transformation should therefore be faster for the biphasic nanoreactor implementation, because of the rate dependence on the catalyst concentration, in the absence of mass transport limitations. However, the chemical environment around the catalytic center is not exactly the same for the two systems: substrate/1-nonanol for the homogeneous system and substrate/polystyrene/1-nonanol for the biphasic one. A comparison of the results obtained for the three different P:Rh ratios (1:1, 2:1 and 4:1) shows an approximately equal reactivity, with complete conversions within ca. 2.5 hours (see Figure S10). Once again, each data point comes from a different experiment and thus errors may be large, preventing a more quantitative kinetics comparison. However, the fact that the biphasic system is not significantly faster than the homogeneous one suggests mass transport limitations. The present cationic-shell nanoreactors are more efficient than the equivalent neutral-shell CCM nanoreactors, since the latter gave quantitative conversions only after ca. 20 h under the same experimental conditions.[11d] We can conclude that the cationic shell allows faster transport of styrene toward the polymer core and/or of the ethylbenzene product back toward the continuous organic phase, relatively to the neutral P(MAA-*co*-PEOMA) shell.

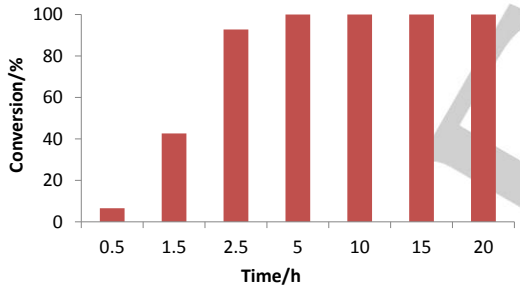

Figure 6. Time dependence of the styrene conversion for the biphasic catalyzed styrene hydrogenation by the **CCM 10%** latex with a P:Rh ratio of 4:1 in 1-nonanol. Each point was generated by an independent experiment (styrene/1-nonanol = 1:9 v/v; styrene/Rh = 200:1; T = 25°C, $p(H_2)$ = 20 bar).

Another important parameter, which indeed motivated the development of this second-generation cationic-shell nanoreactors, is catalyst leaching. It was hoped that reduced lipophilicity of the polycationic P(4VPMe$^+$I$^-$) shell, relative to the neutral-shell first-generation nanoreactors, would reduce the polymer transfer to the organic phase. Indeed, the ICP-MS measurement of the recovered organic phases showed Rh concentrations in most cases much lower than 1 ppm, with an average of 0.24 ppm (see Table S2). There is no significant difference between the average leaching for the CCM (0.25 ppm) and NG (0.22 ppm) catalysts, whereas the measured leaching for the corresponding neutral-shell particle was much greater and architecture-dependent (1.7-2.7 ppm for the CCM[6a, c] and 0.4-1.2 ppm for the NG[7] nanoreactors).

The performance of the **CCM 10%** nanoreactor with a P:Rh ratio of 4:1 was further assessed in terms of catalyst recycling. All the data are collected in Table S3. In order to properly evaluate the catalyst stability and durability, the reaction time in different cycles was initially set at 2.5 h under conditions identical to those of Figure 6 and Table S2, where a fully quantitative conversion was not yet achieved. The results, shown in Figure S11, suggest the presence of a catalyst activation phase, since an essentially quantitative conversion was achieved in all runs after the first recycle. Therefore, in order to more easily detect any catalyst degradation from the conversion *vs.* recycle plot, a second series of recycles was carried out under the same conditions, except for setting the reaction time at 1.5 h. The corresponding results are shown in Figure 7. The presence of an initial catalyst activation phase was now even more evident, but an essentially quantitative conversion was again achieved after the 2nd recycle and up to the 7th recycle. Subsequently, the last two (8th and 9th) recycles gave evidence for a slight decrease of final conversion. In order to verify the reproducibility of these observations, a third recycle run was carried out with a fresh catalytic charge, under the same conditions. The results (Figure S12) indeed rather faithfully reproduced those of Figure 7, including the slight decrease of final conversion after the 7th recycle. This slight decrease may result either from mechanical losses or from catalyst degradation by adventitious oxygen diffusion during the separation of the decanted phases between subsequent cycles. From the quantitative conversions of the recycles (3-7 in Figure 7 and Figure S12), the lower limit of the catalyst TOF in this hydrogenation process is estimated as 133 h^{-1}. The essentially identical DLS and TEM parameters measured for the latex before catalysis and after 1 and 10 catalytic runs indicate that catalytic nanoreactors are stable (see Figure S13). DLS and TEM measurements before and after catalysis were also carried out for the **NG** latex, indicating again no alteration (Figure S14). In addition, the ICP-MS measurement of the Rh concentration in the recovered organic product phases gave even lower values than those indicated above (average of 0.16 ppm) and without any obvious drift for greater recycle numbers.

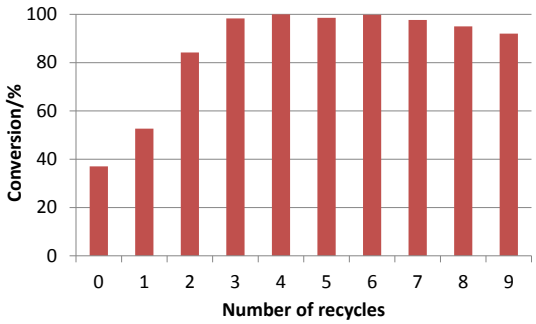

Figure 7. Styrene conversion *vs.* recycle number for the biphasic catalyzed styrene hydrogenation by the **CCM 10%** latex with a P:Rh ratio of 4:1 in 1-nonanol (data in Table S3, runs 11-20). The reaction time for each cycle was 1.5 h. All other conditions were identical to those of Figure 6 (styrene/1-nonanol = 1:9 v/v; styrene/Rh = 200:1; T = 25°C, $p(H_2)$ = 20 bar).

c.2. Hydrogenation of neat styrene.

Since styrene is compatible with the polystyrene core and is thus able to swell the nanoreactors by itself, the hydrogenation

was also tested for the neat substrate, using a styrene/Rh ratio of 5000:1. This reaction was only carried out using the **CCM 10%** nanoreactors, charged with the precatalysts at a P:Rh ratio of 4:1. The conversion *vs.* time study, see Figure 8 (data in Table S4), confirmed the presence of an initial activation phase, since only a 12.1% conversion was achieved after 5 h (average TOF = 120 h^{-1}). However, the conversion was quantitative after 20 h and the slope of the conversion *vs.* time between 5 and 20 h yields an average TOF of ca. 300 h^{-1}. Nine subsequent recycles, with a reaction time of 5 h, demonstrated excellent stability. No strong evidence for an induction phase was shown in this case, probably because the catalyst is already fully activated at the end of the first cycle. For these catalytic runs, the average concentration of Rh leached into the product phase was 0.13 ppm, once again without an obvious drift for high recycle numbers. The corresponding neutral-shell CCM gave a similar TOF for the hydrogenation of neat styrene (ca. 220 h^{-1}) in the first and second run, but leaching was higher (0.3-0.6 ppm) and a loss of activity was observed for the second recycle.[11d]

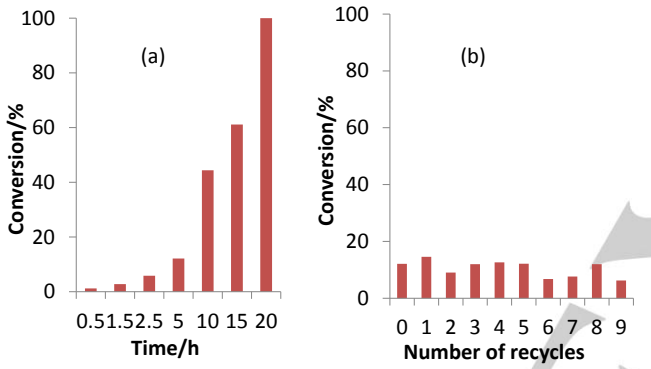

Figure 8. (a) Time dependence of the styrene conversion for the biphasic catalyzed hydrogenation of neat styrene by the **CCM 10%** latex with a P:Rh ratio of 4:1. Each point was generated by an independent experiment (styrene/Rh = 5000:1; T = 25°C, $p(H_2)$ = 20 bar). (b) Recycling under the same conditions as in (a), for t = 5 h.

c.3. Hydrogenation of 1-octene in 1-nonanol and in toluene.

1-Octene is not a good solvent for polystyrene, hence its hydrogenation must be carried out in an organic solvent able to swell polystyrene. This reaction was again carried out only with the **CCM 10%** polymer latex and a 4:1 P:Rh ratio, using identical conditions as for the styrene/1-nonanol studies shown above (substrate concentration of 10% in volume, 25°C at 20 bar of H_2 pressure). The resulting activity was quite similar to that observed for the styrene hydrogenation, leading to a nearly quantitative conversion (97.2%) after 5 h and a quantitative one after 20 h (see Table S5 and Figure S15), with octane as the only observed product and an average leaching of 0.13 ppm.

As stated above, the neutral-shell CCM led to coagulation when the hydrogenations were carried out with toluene as the carrier organic solvent. This phenomenon, due to irreversible particle coupling, was attributed to the formation of species where the Rh atoms are bonded to TPP ligands from different particle cores, which occurs because particle interpenetration is allowed by the neutral shell. In the present case, however, the charged nature of the outer shell blocks the particle interpenetration, as shown above (metal migration study). Indeed, when the hydrogenation of 1-octene catalyzed by the [RhCl(COD)]/**CCM 10%** latex was repeated with use of toluene as organic solvent, the decantation process was equally fast as for the corresponding reaction with 1-nonanol (see Figure S16). The substrate conversion was again quantitative (Table S5) and leaching was again very low (0.08 ppm).

Conclusion

This contribution has presented a new family of triphenylphopshine-functionalized unimolecular amphiphilic polymers with spherical morphology, with either crosslinking at the end of the hydrophobic blocks (core-crosslinked micelles, CCM) or throughout the hydrophobic core (nanogels, NG). They differ from previously described similar polymers by the nature of the outer shell, which is polycationic. These polymers have been obtained by a convergent and well-controlled RAFT polymerization and, after loading with $[RhCl(COD)]_2$, function as efficient nanoreactors for aqueous biphasic hydrogenation of olefins. The performance of these cationic-shell nanoreactors is superior to that of the equivalent polymers with a neutral shell in terms of activity, catalyst stability, recyclability, and catalyst leaching, which can be ascribed to the greater ability of the polycationic shell to confine the nanoreactors in the aqueous phase, while not hurting the mass transport of reactants and products between the continuous organic phase and the nanoreactor core. These nanoreactors (or related ones obtained by the incorporation of other ligand-functionalized monomers) should be suitable to anchor a wide variety of catalytic metals and thus be applied to numerous other catalyzed transformations under aqueous biphasic conditions.

Experimental Section

Materials and methods. All manipulations were performed with Schlenk-line techniques under an inert atmosphere of dry argon. Solvents were dried by standard procedures and distilled under argon prior to use. 4,4'-Azobis(4-cyanopentanoic acid) (ACPA, >98%, Fluka), diethylene glycol dimethacrylate (DEGDMA, 95%, Aldrich), 4-(diphenylphosphino) styrene (DPPS, 97%, Aldrich), 1-octene (>99%, ACROS Organics), *n*-decane (99%, Alfa Aesar), chloro(1,5-cyclooctadiene)rhodium(I) dimer ($[RhCl(COD)]_2$, min. 40.8% Rh, ACROS Organics), 1-nonanol (>99%, TCI), 1,3,5-trioxane (>99%, Aldrich) and iodomethane (MeI, >98%, Sigma) were used as received. 4-Vinyl pyridine (4VP, 95%, Sigma) and styrene (St, 99%, Acros) were distilled under reduced pressure prior to use. The macroRAFT agent R_0-$(4VPMe^+I^-)_{140}$-*b*-S_{50}-SC(S)SPr·34(DMF) (yellow powder, molar mass = 40073 g mol^{-1}) was synthesized in three steps from 4-cyano-4-thiothiopropylsulfanyl pentanoic acid (CTPPA, or R_0-SC(S)SPr with R_0 = $-C(CH_3)(CN)CH_2CH_2COOH$),[18] 4-vinyl pyridine, styrene and methyl iodide as previously described.[12] The DMF content in this product was determined by ^1H NMR in DMSO-d_6 and all attempts to remove the residual 34 molecules of DMF per polymer chain were unsuccessful. Other macroRAFT agents with different number average degrees of polymerization, R_0-$(4VPMe^+I^-)_x$-*b*-S_{50}-SC(S)SPr (x = 56, 72, 150) were prepared by the same procedure using different VP/CTPPA molar ratios. The deionized water used for the syntheses and for the DLS analyses was obtained from a Purelab Classic UV system (Elga Lab-Water).

Characterization Techniques

NMR spectroscopy. All nuclear magnetic resonance spectra were recorded in 5 mm diameter tubes at 297 K on a Bruker Avance 400 spectrometer. The ^{1}H and ^{31}P chemical shifts were determined using the residual peak of the deuterated solvent as internal standard and are reported in ppm (δ) relative to tetramethylsilane. Peaks are labelled as singlet (s), doublet (d), triplet (t), quadruplet (q), multiplet (m) and broad (br). For the CCM characterization, the chemical shift scale was calibrated on the basis of the solvent peak (δ 2.50 for DMSO-d_6, 4.79 for D_2O, 7.26 for $CDCl_3$), and 1,3,5-trioxane (δ 5.20) was used as an integration reference. For the synthesis of the P4VP macroRAFT agent, the monomer conversion was followed by ^{1}H NMR spectroscopy (300 MHz Bruker) in DMSO-d_6 at room temperature by the relative integration of the protons of the internal reference (1,3,5-trioxane) at 5.2 ppm and the vinylic protons of 4VP (at 5.4 and 5.9 ppm).

Dynamic light scattering (DLS). The intensity-average diameters of the latex particles (D_z) and the polydispersity index (PDI) were obtained on a Malvern Zetasizer NanoZS equipped with a He-Ne laser (λ = 633 nm), operating at 25 °C. Samples were analyzed after dilution with deionized water, either unfiltered or after filtration through a 0.45 µm pore-size membrane. Zeta potential (ζ) measurements were also conducted on the same instrument by measuring the electrophoretic mobility.

Transmission electron microscopy (TEM). The morphological analyses of the copolymer nano-objects were performed at the Centre de Microcaractérisation Raimond Castaing (Toulouse, France) with a JEOL JEM 1400 transmission electron microscope working at 120 kV. Diluted latex samples were dropped on a formvar/carbon-coated copper grid and dried under vacuum for 24 hours. The diameter distributions of the CCM and NG particles were obtained with help of the ImageJ software, using images with 100-300 particles.

Gas chromatography (GC). The GC test of remained substrates and products in the organic layer after catalysis was conducted by Shimadzu GC 2014 chromatograph equipped with a SLB 5ms capillary column (30 m×0.32 mm; 0.23 µm film thickness) and a flame ionization detector (FID), using helium as carrier gas. The peak assignment was assisted by a separate GC/MS analysis.

High resolution inductive couple plasma – mass spectrometry (ICP-MS). The rhodium catalyst leaching in the organic phase was quantified by high resolution ICP/MS on a XR Thermo Scientific Element. For the sample preparation, the recovered organic phase was diluted into water using a 10^4 volumetric dilution factor, high enough to ensure complete dissolution. In practice, a 100 mL volumetric flask was filled at 2/3 with Milli-Q water, then 10 µL of the organic product phase were introduced using a precision pipette. Borders were rinsed and the flask was introduced into an ultrasound bath for 15 min. The dilution was then completed with Milli-Q water to the 100 mL mark, followed by further sonication for 45 min. Standards were prepared using [RhCl(COD)]2 and triphenylphosphine dissolved in toluene, attaining Rh concentrations in aqueous solution in the 1–100 ppt range. The relative standard deviation on the measurements used for the calibration was 3%.

Preparation of latexes of the R_0-(4VPMe$^+$I$^-$)$_a$-*b*-S_b-*b*-(S_{1-x}-*co*-DPPS$_x$)$_c$-SC(S)SPr amphiphilic copolymers. The synthesis of all latexes of this type followed the same procedure, which is detailed here only for the product with a,b,c,x = 140,50,300,0.1 (**diblock 10%**). A stock solution of water ACPA/$NaHCO_3$ was prepared with 5 mL of H_2O and dissolution of ACPA/$NaHCO_3$ (0.10 g / 0.10 g), [ACPA] = 71.4 mmol L^{-1}. The [R_0-(4VPMe$^+$I$^-$)$_{140}$-*b*-S_{50}-SC(S)SPr]·34(DMF) macroRAFT agent (2 g, 49.9 µmol) was dissolved in 15 mL of degassed water under Ar in a Schlenk tube to afford a pale yellow dispersion. To this solution was added 1,3,5-trioxane (11.9 mg, 0.13 mmol, used as ^{1}H NMR internal reference), degassed styrene (1.55 mL, 1.40 g, 13.48 mmol, 270 equiv. per chain) and DPPS (0.43 g, 1.50 mmol, 30 equiv. per chain). A portion of the degassed ACPA/$NaHCO_3$ stock solution (1.4 mL, 28.02 mg ACPA, 0.1 mmol) was then added and the resulting reaction mixture was stirred at 80 °C for 3 h, yielding a white opalescent stable dispersion. The resulting polymer has a theoretical molar mass of 76847 g mol^{-1}. The weight percent polymer in the latex is 18.9%.

Using the same amounts of [R_0-(4VPMe$^+$I$^-$)$_{140}$-*b*-S_{50}-SC(S)SPr]·34(DMF), ACPA solution, water and trioxane but different amounts of degassed styrene and DPPS led to latexes of the product with different DPPS content (5% or 20%) in the hydrophobic block. **Diblock 5%** (a,b,c,x = 140,50,300,0.05): styrene (1.64 mL, 1.48 g, 14.25 mmol, 285 equiv. per chain), DPPS (0.22 g, 0.75 mmol, 15 equiv. per chain), $M_{n,th}$ = 74090 g mol^{-1}, polymer content = 18.4% (w/w). **Diblock 20%** (a,b,c,x = 140,50,300,0.2): styrene (1.38 mL, 1.25 g, 13.48 mmol, 240 equiv. per chain), DPPS (0.86 g, 3.0 mmol, 60 equiv. per chain), $M_{n,th}$ = 82361 g mol^{-1}, polymer content = 20.0 % (w/w).

Latexes with other a,b,c,x values (as reported in Table S1) were obtained by the same procedure from the appropriate R_0-(4VPMe$^+$I$^-$)$_a$-*b*-S_b-SC(S)SPr macroRAFT agents, using suitable molar amounts of styrene and DPPS for the chain extension.

Cross-linking of the amphiphilic copolymers. Preparation of R_0-(4VPMe$^+$I$^-$)$_a$-*b*-S_b-*b*-(S_{1-x}-*co*-DPPS$_x$)$_c$-*b*-(S_{1-y}-*co*-DEGDMA$_y$)$_d$-SC(S)SPr (CCM). The same general procedure was used for all CCM particles and will be described in detail only for the product with a,b,c,d,x,y = 140,50,300,140,0.1,0.1 (**CCM 10%**). To the Schlenk tube containing the entire aqueous suspension of the R_0-(4VPMe$^+$I$^-$)$_{140}$-*b*-S_{50}-*b*-($S_{0.9}$-*co*-DPPS$_{0.1}$)$_{300}$-SC(S)SPr (**diblock 10%)** polymer, prepared as described in the previous section, were successively added degassed styrene (0.702 g, 6.74 mmol, 135 equiv. per chain), DEGDMA (0.17 mL, 0.18 g, 0.75 mmol, 15 equiv. per chain), and 1.4 mL of the degassed ACPA/$NaHCO_3$ stock solution (28.02 mg ACPA, 0.1 mmol). The resulting reaction mixture was stirred at 80 °C for 8.5 h. The monomer conversions were 91.0% for styrene and 100% for DEGDMA (by ^{1}H NMR in DMSO-d_6). The final polymer has a theoretical molar mass of 93278 g mol^{-1} and the polymer content in the latex is 20.6 % w/w ([TPP] = 73.8 µmol/mL).

The same procedure, starting from the latex of either **diblock 5%** or **diblock 20%**, gave a latex of **CCM 5%** or **CCM 20%**, respectively. For **CCM 5%**: styrene (0.72 mL, 0.656 g, 6.30 mmol, 126 equiv. per chain), DEGDMA (0.16 mL, 0.17 g, 0.70 mmol, 14 equiv. per chain) and degassed ACPA/$NaHCO_3$ stock solution (1.4 mL, 28.02 mg ACPA, 10.0 µmol); stirring at 80 °C for 4 h; conversions = 99.0% for styrene and 100% for DEGDMA; $M_{n,th}$ = 90508 g mol^{-1}; polymer content in the latex = 20.2 % (w/w) ([TPP] = 40.3 µmol/mL). For **CCM 20%**: styrene (0.72 mL, 0.655 g, 6.29 mmol, 126 equiv. per chain), DEGDMA (0.16 mL, 0.17 g, 0.75 mmol, 14 equiv. per chain) and the degassed ACPA/$NaHCO_3$ stock solution (1.4 mL, 28.02 mg ACPA, 10.0 µmol); stirring at 80 °C for 4 h; conversions were nearly 100 % for styrene and 100% for DEGDMA; $M_{n,th}$ = 98878 g mol^{-1}; polymer content in the latex = 21.6 % (w/w) ([TPP] = 148.7 µmol/mL).

Latexes of CCM particles with other a,b,c,d,x,y values (as reported in Table S1) were obtained by the same procedure from the appropriate amphiphilic diblock precursors, using suitable molar amounts of styrene and DEGDMA for the crosslinking step.

Preparation of a latex of the amphiphilic nanogel copolymer R_0-(4VPMe$^+$I$^-$)$_{140}$-*b*-S_{50}-*b*-(S_{426}-*co*-DPPS$_{30}$-*co*-DEGDMA$_{15}$)-SC(S)SPr (NG). To the Schlenk tube containing an aqueous suspension of [R_0-(4VPMe$^+$I$^-$)$_{140}$-*b*-S_{50}-SC(S)SPr]·34(DMF) polymer (0.5 g, 12.5 µmol), prepared as described previously,[12] in 6 mL of distilled water were added 1,3,5-trioxane (10.6 mg, 0.12 mmol) and degassed styrene (0.62 mL, 56.2 mg, 5.39 mmol), DPPS (0.109 g, 0.38 mmol) and DEGDMA (42 µL , 45.4 mg, 187.8 µmol), and finally the degassed ACPA/$NaHCO_3$ stock solution (0.38 mL, 7.5 mg ACPA, 27.1 µmol). The reaction mixture was stirred at 80°C for 4 h. The NMR (DMSO-d_6) indicated the complete conversion of all monomers. The final polymer has a theoretical molar mass of 96732 g

mol^{-1} and the latex has a polymer content of 16.0 % w/w ([TPP] = 53.2 µmol/mL).

General procedure for metal complexation to the phosphine ligand within polymer core. All metal complexation reactions were carried out using the same procedures, which is described here in detail for the CCM 10% polymer with a P:Rh ratio of 4:1. In a Schlenk tube was added 1 mL of the **CCM 10%** polymer latex (containing 73.8 µmol of TPP) and 3 mL of H_2O. Toluene (3 mL) was added and the mixture was stirred for 5 min, resulting in the CCM particle core swelling. Then a separately prepared solution of $[RhCl(COD)]_2$ (4.6 mg, 9.23 µmol) in toluene (1 mL) was added to the latex and the mixture was vigorously stirred at room temperature, stopping the stirring at regular intervals (decantation was rapid, < 1 min) to assess the reaction progress. The aqueous phase progressively became yellow while the toluene phase became completely colorless after 30 minutes of stirring. For the procedure with a P:Rh ratio of 1:1, since a slight excess of $[RhCl(COD)]_2$ was used to ensure quantitative complexation of the TPP ligands, the resulting latex was extracted by toluene until the organic phase was colorless to remove the metal precursor excess. The measured latex volume was 5.8 mL ([TPP] = 12.7 µmol/mL).

General procedure for the aqueous biphasic catalytic hydrogenations. (a) Substrate/Rh = 200. In a vial containing a magnetic stirrer was added 1 mL of the Rh-charged latex (CCM 10%, CCM 5% or NG 10%), prepared as described in the previous sections. The desired amount of substrate (styrene or 1-octene), mixed with 1-nonanol or toluene (10% v/v), was layered on top of the latex. **(b) Styrene/Rh = 5000.** In a vial containing a magnetic stirrer was added 0.4 mL of **CCM 10%** (5.09 µmol of TPP; 1.27 µmol of Rh) and then neat styrene (0.73 mL, 664 g, 6.37 mmol). For all experiments, whatever the substrate/Rh ratio, decane (internal standard) was then added to the organic layer (substrate/decane molar ratio ≈ 4). The vial was then placed inside an autoclave, which was subsequently charged with dihydrogen (20 bar), placed in a thermostatic oil bath and stirred at 1200 rpm. At the set reaction time, the stirring was stopped, the autoclave was vented and the vial was taken out under argon. The latex decantation was rapid (< 1 min). An aliquot of the organic phase was used for the ICP-MS analysis of the Rh leaching. After phase separation, the latex was extracted with diethyl ether (3×0.3 mL). The combined organic phases were used for the GC analysis. For the recycling experiments, a fresh substrate solution (same amounts as in the initial run) was added to the same vial, followed by reaction and product separation according to the same protocol.

Acknowledgements

We are grateful to the Centre National de la Recherche Scientifique (CNRS), to the Agence Nationale de la Recherche (project BIPHASNANOCAT, grant number ANR-11-BS07-025-01) and to the Institut Universitaire de France (IUF) for financial support. We are also grateful to the China Scholarship Council for a Ph.D. fellowship to HW.

Keywords: Polyelectrolyte • RAFT polymerization • Polymerization-induced self-assembly • Poly(1-methyl-4-vinylpyridinium iodide) • Catalytic nanoreactors

[1] B. Cornils and W. A. Herrmann in *Aqueous Phase Organometallic Catalysis*, *Vol.* Wiley-VCH, Weinheim, **1997**.

[2] C. W. Kohlpaintner, R. W. Fischer and B. Cornils, *Appl. Catal., A* **2001**, *221*, 219-225.

[3] A. Behr in *Thermomorphic solvent systems*, *Vol. 1* Eds.: B. Cornils, W. A. Herrmann, I. T. Horvath, W. Leitner, S. Mecking, H. Olivier-Bourbigou and D. Vogt), Wiley-VCH, Weinheim, Germany, **2005**, pp. 327-329.

[4] a) G. Oehme in *Micellar systems*, Eds.: B. Cornils and W. A. Herrmann), Wiley-VCH, Weinheim, Germany, **2004**, pp. 256-271; b) M. N. Khan, *Micellar Catalysis*, CRC Press, **2006**, p. 464 pp.

[5] a) P. Cotanda, N. Petzetakis and R. K. O'Reilly, *MRS Communications* **2012**, *2*, 119-126; b) A. Lu and R. K. O'Reilly, *Current Opinion in Biotechnology* **2013**, *24*, 639-645; c) *Effects of Nanoconfinement on Catalysis*, R. Poli (Ed.), Springer, New York, **2017**.

[6] a) X. Zhang, A. F. Cardozo, S. Chen, W. Zhang, C. Julcour, M. Lansalot, J.-F. Blanco, F. Gayet, H. Delmas, B. Charleux, E. Manoury, F. D'Agosto and R. Poli, *Chem. Eur. J.* **2014**, *20*, 15505–15517; b) E. Manoury, F. Gayet, F. D'Agosto, M. Lansalot, H. Delmas, C. Julcour, J.-F. Blanco, L. Barthe and R. Poli in *Core-cross-linked micelles and amphiphilic nanogels as unimolecular nanoreactors for micellar-type, metal-based aqueous biphasic catalysis*, (Ed. R. Poli), Springer, New York, **2017**, pp. 147-172; c) A. F. Cardozo, C. Julcour, L. Barthe, J.-F. Blanco, S. Chen, F. Gayet, E. Manoury, X. Zhang, M. Lansalot, B. Charleux, F. D'Agosto, R. Poli and H. Delmas, *J. Catal.* **2015**, *324*, 1-8.

[7] E. Lobry, A. F. Cardozo, L. Barthe, J.-F. Blanco, H. Delmas, S. Chen, F. Gayet, X. Zhang, M. Lansalot, F. D'Agosto, R. Poli, E. Manoury and C. Julcour, *J. Catal.* **2016**, *342*, 164-172.

[8] a) J. Chiefari, Y. K. Chong, F. Ercole, J. Krstina, J. Jeffery, T. P. T. Le, R. T. A. Mayadunne, G. F. Meijs, C. L. Moad, G. Moad, E. Rizzardo and S. H. Thang, *Macromolecules* **1998**, *31*, 5559-5562; b) D. J. Keddie, G. Moad, E. Rizzardo and S. H. Thang, *Macromolecules* **2012**, *45*, 5321-5342.

[9] a) B. Charleux, G. Delaittre, J. Rieger and F. D'Agosto, *Macromolecules* **2012**, *45*, 6753-6765; b) S. L. Canning, G. N. Smith and S. P. Armes, *Macromolecules* **2016**, *49*, 1985-2001; c) M. Lansalot, J. Rieger and F. D'Agosto in *Polymerization-Induced Self-Assembly: The Contribution of Controlled Radical Polymerization to The Formation of Self-Stabilized Polymer Particles of Various Morphologies*, Eds.: L. Billon and O. Bourisov), John Wiley & Sons, Inc., **2016**, pp. 33-82; d) F. D'Agosto, J. Rieger and M. Lansalot, *Angewandte Chemie-International Edition* **2020**, *59*, 8368-8392.

[10] a) T. Terashima, M. Kamigaito, K.-Y. Baek, T. Ando and M. Sawamoto, *J. Am. Chem. Soc.* **2003**, *125*, 5288-5289; b) R. K. O'Reilly, C. J. Hawker and K. L. Wooley, *Chemical Society Reviews* **2006**, *35*, 1068-1083; c) Y. Liu, Y. Wang, Y. F. Wang, J. Lu, V. Pinon and M. Weck, *Journal of the American Chemical Society* **2011**, *133*, 14260-14263; d) T. Terashima in *Polymer Microgels for Catalysis*, (Ed. H. F. Mark), John Wiley & Sons, Inc., **2013**, p. 10.1002/0471440264.pst0471440590.

[11] a) S. Chen, A. F. Cardozo, C. Julcour, J.-F. Blanco, L. Barthe, F. Gayet, B. Charleux, M. Lansalot, F. D'Agosto, H. Delmas, E. Manoury and R. Poli, *Polymer* **2015**, *72*, 327-335; b) R. Poli, S. Chen, X. Zhang, A. Cardozo, M. Lansalot, F. D'Agosto, B. Charleux, E. Manoury, F. Gayet, C. Julcour, J.-F. Blanco, L. Barthe and H. Delmas, *ACS Symp. Ser.* **2015**, *1188*, 203-220; c) S. Chen, F. Gayet, E. Manoury, A. Joumaa, M. Lansalot, F. D'Agosto and R. Poli, *Chem. - Eur. J.* **2016**, *22*, 6302 – 6313; d) A. Joumaa, S. Chen, S. Vincendeau, F. Gayet, R. Poli and E. Manoury, *Mol. Cat.* **2017**, *438*, 267-271.

[12] H. Wang, L. Vendrame, C. Fliedel, S. Chen, F. Gayet, E. Manoury, X. Zhang, M. Lansalot, F. D'Agosto and R. Poli, *Macromolecules (Washington, DC, U. S.)* **2020**, *53* 2198-2208.

[13] S. Chen, E. Manoury, F. Gayet and R. Poli, *Polymers* **2016**, *8*, 26.

[14] A. J. Naaktgeboren, R. J. M. Nolte and W. Drenth, *Journal of the American Chemical Society* **1980**, *102*, 3350-3354.

[15] E. Kwaskowska-Chęć, A. M. Trzeciak and J. J. Ziolkowski, *Reaction Kinetics and Catalysis Letters* **1984**, *26*, 21-24.

[16] a) Y. D. Lu, Y. H. Wang and Z. L. Jin, *Chinese Chemical Letters* **2010**, *21*, 1067-1070; b) M. M. Niu, Y. H. Wang, P. Chen, D. J. Du, J. Y. Jiang and Z. L. Jin, *Catalysis Science & Technology* **2015**, *5*, 4746-4749; c) J. L. Castelbou, E. Breso-Femenia, P. Blondeau, B. Chaudret, S. Castillon, C. Claver and C. Godard, *ChemCatChem* **2014**, *6*, 3160-3168; d) D. J. M. Snelders, N. Yan, W. Gan, G. Laurenczy and P. J. Dyson, *ACS Catalysis* **2012**, *2*, 201-207; e) B. L. Tran, J. L. Fulton, J. C. Linehan, J. A. Lercher and R. M. Bullock, *Acs Catalysis* **2018**, *8*, 8441-8449.

[17] M. Ibrahim, M. M. Wei, E. Deydier, E. Manoury, R. Poli, P. Lecante and K. Philippot, *Dalton Trans.* **2019**, *48*, 6777-6786.

[18] a) X. Xu, A. E. Smith, S. E. Kirkland and C. L. McCormick, *Macromolecules* **2008**, *41*, 8429-8435; b) T. Boursier, I. Chaduc, J.

Rieger, F. D'Agosto, M. Lansalot and B. Charleux, *Polymer Chemistry* **2011**, *2*, 355-362.

Entry for the Table of Contents

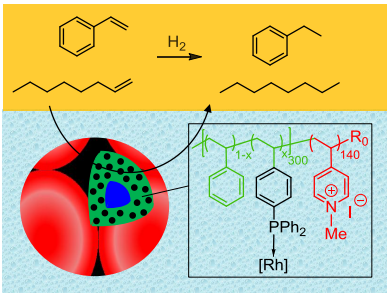

Stable latexes of size-controlled spherical and unimolecular polymers, made of a crosslinked and phosphine-functionalized hydrophobic core and a poly(N-methyl-4-vinylpyridinium) shell, are efficient nanoreactors for rhodium-catalyzed hydrogenation under aqueous biphasic conditions with excellent recyclability and negligible leaching.